In general, the minimum MSE is sensitive to the parameter choice with the most sensitivity shown for l and least sensitivity for k. A small change in l (0.1 for cloudiness and 10 km for spatial) typically degrades the MSE by 10% or more. One exception is the combination of the SE model and spatial covariance which produce MSE surfaces that are less sensitive to a range of parameters, for example a 40 km difference in l only raises the MSE by 10%.

Large d values for the UASIBS model indicate that the estimated variance from only the clear days is too low. This is because UASIBS suppresses many clouds or slight variations on clear days. An example of this on a cloudy day is shown in Fig. 2. A value of $d < 1$ for the SE model indicates that the model tends to overestimate the variance on cloudy days as a result of the tendency to overproduce clouds even at times that should be clear.

Our proposed tuning process is computationally intensive but manageable; computation for one set of (k, l, d) and one cross-validation set using 24 cores of two Intel Xeon E5-2690 v3 processors takes nearly 10 min. Thus, to tune over the six cross-validation sets, three choices of k, ten choices of both l and d, spatial and cloudiness correlation parameterizations, and the SE and UASIBS models would take nearly 7 weeks on a single 24 core machine. It would take a typical 4 core laptop or desktop nearly a year to perform the same tuning. To speed up this tuning, the bulk of the operations were converted to GPU code which decreased the run-time for a single parameter set over the test data to 5 min using a single GPU. We used the University of Arizona's El Gato supercomputer, which has 140 NVIDIA K20x GPUs, to perform the tuning in a matter of days. Once tuning is complete, OI can be computed in under five seconds for each image.

7. Results and discussion

We compute the OI analysis on each of the images in the verification data set using optimal parameters found in Section 6. First, we compute the analysis of the verification data by only withholding the NREL MIDC GHI sensor at the University of Arizona, and later we calculate errors while performing six fold cross-validation over the sensors.

Scatter plots of predicted versus measured values at the NREL MIDC sensor using cloudiness covariance are shown in Fig. 4. In the clear-sky index scatter plots, we see that the UASIBS model under-predicts clouds while the SE model over-predicts clouds. It is interesting to note that the UASIBS model does not predict clear-sky index values between 0.6 and 0.8, and that OI helps to fill in this gap. The GHI scatter plots show that the analysis performs well and is more tightly scattered around the $y = x$ line with minimal bias. It is especially striking to note how well OI improves the GHI estimates for the SE model. Figs. 2 and 4 also demonstrate that OI is not simply a bias correction applied to the whole background because the analysis is not a linear (or even polynomial) function applied to the background values. This is especially evident in the scatter plot of GHI for the SE model (lower right of Fig. 4).

We compute the mean bias error (MBE), mean absolute error (MAE), and root mean squared error (RMSE) over the verification data with 5 min average sensor data and "instantaneous" satellite estimates. For RMSE, the square root is computed after all averaging computations. The errors in GHI when only the NREL MIDC sensor was withheld from the OI routine and converting clear-sky index to GHI using the sensor's clear-sky profile are shown in Table 2.

To calculate the errors over the cross-validation sensors in order to validate OI at locations not included in the algorithm, we averaged over the withheld sensors, the cross-validation runs, and the verification images. Fig. 5 shows the reduction in errors for the UASIBS and SE models using cloudiness covariance for the analysis errors as compared to the background errors. Table 3 presents the errors for the background and analysis computed with each covariance method for the UASIBS and SE models, respectively. Analyzing Figs. 4 and 5 and Tables 2 and 3, we see that the SE model initially has a large bias that is corrected in the analysis. This also leads to large MAE and RMSE relative improvements of 68% and 50%, respectively. The analysis using the best covariance parameterization for UASIBS had a RMSE relative improvement of 16%.

Furthermore, it is interesting to see that the errors after optimal interpolation are similar for both the UASIBS and SE models. We interpret this as evidence that one can use the relatively simple

Table 2
Error statistics for the NREL MIDC sensor on the University of Arizona campus. The analysis was computed with only the MIDC sensor withheld and averaged over the verification data set, and cloudiness covariance was used. Both the UASIBS and SE models show improvements and have a similar analysis RMSE. Units are W/m^2.

	MBE	MAE	RMSE
UASIBS analysis	4.16	27.2	71.1
UASIBS background	20.7	38.8	98.8
SE analysis	11.2	36.0	72.7
SE background	−86.1	107	140

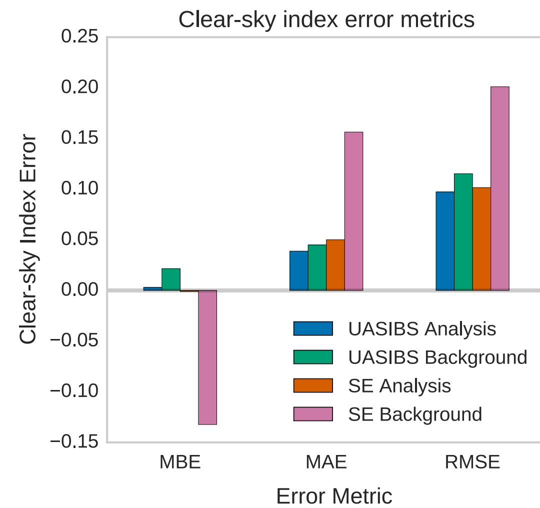

Fig. 5. Clear-sky index cross-validation error statistics for the UASIBS and SE models before (background) and after (analysis) performing OI using cloudiness covariance with the optimal parameters listed in Table 1. The error statistics were computed by averaging over the withheld sensors, the cross-validation runs, and the verification times. The SE model initially has a large bias that is corrected by the analysis. After analysis, both the UASIBS and SE models have similar RMSE.

Table 3
Clear-sky index error statistics using the UASIBS and SE models with cloudiness, spatial, or empirical covariance parameterizations. Errors are calculated by averaging over the withheld sensors, cross-validation runs, and verification images. OI using any of the covariance methods improves upon the background for both models. All errors are in units of clear-sky index.

	MBE	MAE	RMSE
UASIBS model			
Cloudiness analysis	0.003	0.039	0.097
Spatial analysis	0.004	0.038	0.099
Empirical analysis	0.000	0.043	0.105
Background	0.022	0.045	0.115
SE model			
Cloudiness analysis	−0.001	0.050	0.102
Spatial analysis	−0.005	0.051	0.105
Empirical analysis	−0.001	0.051	0.106
Background	−0.132	0.156	0.201